IAMG'06 Int. Assoc. for Mathematical Geology
XI[th] International Congress
Université de Liège - Belgium

ASTER DEMs for volcano topographic mapping: accuracy and limitations

M. Kervyn [1]*, R. Goossens[2], P. Jacobs[1], G.G.J. Ernst[1]

[1] *Mercator & Ortelius Research Centre for Eruption Dynamics, Department of Geology and Soil Sciences, Ghent University, Krijgslaan 281/S8,B- 9000 Ghent, Belgium.*
[2] *Remote Sensing and Photogrammetry Unit, Department of Geography, Ghent University, Krijgslaan 281/S8, B-9000 Ghent, Belgium*
[*] *Corresponding Author: Matthieu.KervynDeMeerendre@UGent.be*

ABSTRACT: High spatial resolution topographic data is essential to assist volcanic field work, for volcano morphology analyses, and for hazard modelling of volcanic flow processes. The stereoscopic capability of ASTER data provides the opportunity to derive DEMs at a spatial resolution of 15 m for the many regions lacking accurate topographic maps. Case studies of digital photogrammetry applications with ASTER data are presented for Mauna Kea and Oldoinyo Lengai volcanoes, in Hawaii and Tanzania, respectively. The accuracy of the results is quantitatively assessed against high-resolution topographic datasets and compared with the new SRTM data. High accuracy Ground Control Points (GCPs), extracted from a 1:24.000 topographic map, allowed good absolute orientation of the ASTER DEM for Mauna Kea. Small errors in the image matching process, due to low image contrast, however, resulted in small-scale artefacts. Compared with a topographic dataset with 10 m resolution, an RMSE of 13 m is obtained, twice the error obtained with the 30 m SRTM DEM (i.e. 6 m). Using GPS data acquired for other purposes, the accuracy of the absolute orientation for the Lengai ASTER DEM is poorer. The ASTER DEM, however, proves accurate for relative elevation measurements of features higher than 100 m. ASTER offers the possibility to derive DEMs with a resolution up to 6 times higher than that provided by SRTM. It is nevertheless limited by cloud coverage and requires high accuracy GPS data points (GCPs), specifically collected in the field for accurate absolute orientation. The problem of small-scale topographic artefacts can be solved by multiple DEMs combination or by low pass filtering, the latter inducing a loss of effective spatial resolution.

Keywords: Digital Elevation Models (DEMs), Oldoinyo Lengai, Mauna Kea, volcano topography, accuracy, ASTER, SRTM, remote sensing, volcano morphometry

1. Introduction

The majority of historically-active volcanoes (Simkin & Siebert, 1994) remains poorly known and irregularly monitored. Aerial photographs and good quality topographic maps are very difficult to obtain for many volcanically-active regions (e.g. Kervyn et al., 2006b). Accurate and detailed topographic datasets are however essential to map and to study volcano morphology, to assess hazards and to model volcanic processes and associated risks (e.g. Stevens et al., 2002). The need of high-resolution topographic data is a common issue to all geohazard research on landslides, mudflows, avalanches, active faults, flood modelling and diverse volcanic hazards.
Remote sensing (RS) from space-borne sensors now provides the most accurate digital elevation datasets with a worldwide coverage. Here we assess with 2 case studies the accuracy

of DEM derived from ASTER stereo-scenes using digital photogrammetry techniques, in comparison with topographic maps and/or SRTM DEM (Rodríguez et al., 2006). ASTER and SRTM DEMs have both the potential to provide DEMs for most of the world at a resolution of 30 m at low or no cost. Deriving ASTER DEM require to have Ground Control Points (GCPs) to calibrate the data whereas the SRTM data is provided as a fully processed DEM. Comparison of these datasets allows identification of their advantages and limitations in order to select the best suitable dataset for a specific application.

2. Data set

The *Advanced Spaceborne Thermal Emission and Reflection Radiometer (ASTER)* is a medium-to-high spatial resolution, multispectral imaging system flying aboard TERRA, a satellite launched in December 1999 as part of NASA's Earth Observing System program (Pieri & Abrams, 2004). ASTER repetitively acquires along-track stereoscopic images at 15 m spatial resolution for deriving DEMs. Using few test cases, Hirano et al. (2003) suggested that the root mean square error (RMSE) in ASTER DEM elevations ranges from ± 7 m to ± 15 m, depending on GCPs and image quality.

ASTER DEMs are derived using standard photogrammetry techniques, computed here with the software *Virtuozo 3*. The relative orientation (i.e. image-to-image co-referencing) is computed by automatic recognition of textural patterns common on the 2 scenes. Orientation's accuracy depends on contrast within images. Absolute orientation is obtained by locating a minimum of 6 GCPs on both images. The availability and accuracy of high-quality GCPs that can precisely be located on the ASTER stereo-pair determine the accuracy at the absolute orientation stage. After relative and absolute orientation, each pixel of the ASTER image is matched with the corresponding pixel on the other image of the pair. The precision in matching depends on textural contrast around the pixel: matching will be especially poor within areas with homogeneous pixel intensity (e.g. water surface). Combining the matching procedure and the parallax parameters estimated via the relative and absolute orientation permit to derive a DEM at a resolution of 15 m at best, as well as an ortho-rectified ASTER band 3 image.

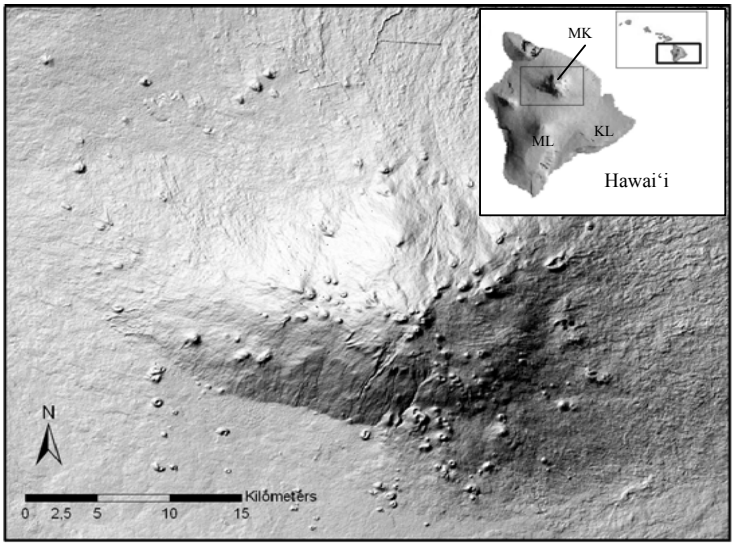

Fig. 1 Shaded relief of Mauna Kea cone field derived from SRTM30 DEM. Inset shows the Big Island of Hawai'i and locations of Mauna Kea (MK), Mauna Loa (ML) and Kilauea (KL).

3. Mauna Kea

The first test case, Mauna Kea (MK) shield volcano (Fig. 1), illustrates many large volcanoes covered with numerous small craters, volcanic lakes, domes and cones of similar spatial scale. The MK cone field is scrutinized because it is one of few such places where an independent high-accuracy dataset is readily available in order to test the accuracy of the ASTER DEM together with the SRTM DEM at 30 m resolution.

3.1. Data processing

Bands 3N and 3B of an ASTER L1B scene, acquired on December 5, 2000, was processed to produce a DEM of MK. Absolute orientation was achieved using 12 GCPs extracted from 1:24,000 scale USGS topographic maps. The DEM was produced at 30 m resolution, to avoid small-scale artefacts obtained when using 15 m resolution. The vertical RMS error at the 12 GCPs was ~6 m, whereas the horizontal RMSE for these points was below 25 m (Table 1). A trade-off had to be found between the high resolution needed in the matching process to render small topographic features (e.g. scoria cone craters) and the increasing proportion of pixels affected by errors. Optimal results were obtained for a matching interval of 3 pixels. To correct pixel values where the DEM computed an unreasonably high slope angle (i.e. wells and peaks) above 45° (i.e. upper limit expected in MK area), these were replaced by the value from a DEM processed with a matching interval of 7 pixels.

a. Parameter	*Mean*	*Standard Deviation*	*RMSE*
dX (m)	17.5	12.6	21.3
dY (m)	23.4	15.1	27.5
dZ (m)	5.2	3.3	6.1

b. GCP	dX (m)	dY (m)	dZ (m)
1	5.6	-43.2	6.0
2	-5.2	25.3	0.6
3	-29.9	-12.0	-6.5
4	6.6	-45.2	-5.7
5	17.7	11.0	-0.2
6	-6.8	-16.0	4.4
7	30.3	16.5	-10.4
8	-21.9	48.3	-9.1
9	22.2	5.7	6.2
10	15.6	-6.5	3.2
11	4.8	-29.5	8.3
12	-43.7	21.0	1.7

Table 1 General (a) and per GCP (b) distribution of errors in x, y and z for the absolute orientation of the ASTER stereo-pair for Mauna Kea. This set of 12 GCPs was the best trade-off between the need for a small overall RMSE and the need for GCPs to be well spread over the entire scene in x, y and z directions, in order to constrain the absolute orientation of all parts of the scene. The RMS error is less than half a pixel size in the z direction but is over 1 pixel in horizontal directions.

3.2. Accuracy assessment

The accuracy of ASTER DEMs was evaluated using a 10 m resolution DEM interpolated from digitised contour lines of the USGS topographic maps. The mean absolute difference between the two DEMs was of 11 m (90% of errors ranging between -18 m and +29 m). Based on 218 control points selected randomly within the study area, the topographic map DEM taken as a reference, we obtained a vertical RMS error of 13 m. In comparison, the same calculation for the 30 m SRTM DEM returned a vertical RMSE of 6 m. Errors in the ASTER DEM are attributed to the low spectral contrast in band 3 and to a lack of precise GCPs on the upper flanks. Part of the errors in both ASTER and SRTM DEM is also attributed to the fact that they are not corrected for the vegetation height.

Visual shaded relief analysis (Fig. 2) illustrates that the ASTER DEM provides a representation with fine-scale artefacts caused by errors in images matching. The ASTER DEM does however render, fairly realistically, topographic variations larger than 3 pixels (90 m) such as the occurrence of craters. The finest topographic features (i.e. small gullies) are however obliterated at 30 m resolution. In comparison, the SRTM at 90 m resolution gives a much smoother representation of the volcanic cones, making it less suitable for quantitative estimates of their size and height.

Height estimation for small volcanic cones, of interest to volcanologists (e.g. Riedel et al., 2003), is chosen here as a suitable generic test for the potential of using the respective DEMs to quantitatively assess the geometry of small geo-features at high resolution. The results can

be extrapolated to other features of interest in geohazards with similar horizontal and vertical scale such as landslide scarps and deposits, explosion craters, and river valleys.

The heights of 40 MK scoria cones, ranging from 20 to 200 m, were independently extracted from topographic maps, SRTM DEM and ASTER DEM. On the ASTER DEM, the height estimates for 65% of cones range from 80% to 110% of the validation height value. The occurrence of high underestimation (>30%, 25% of the cases) is related to small cone height, irregular cone base elevation and low image contrast inducing matching errors. SRTM30 provides smaller discrepancies: for 50% of cones, the 30 m SRTM height estimate is within 10% of the estimate from the 10 m DEM derived from topographic maps. High discrepancy values tend to affect only cones less than 100 m high. When the SRTM90 DEM is used, cone height estimates are significantly lower with an average underestimation of 36%, discrepancies being larger for smaller cones. These discrepancies are consistent with simulations of the smoothing effect of DEM resolution decrease upon spatial measurements (see Kervyn et al., 2006a).

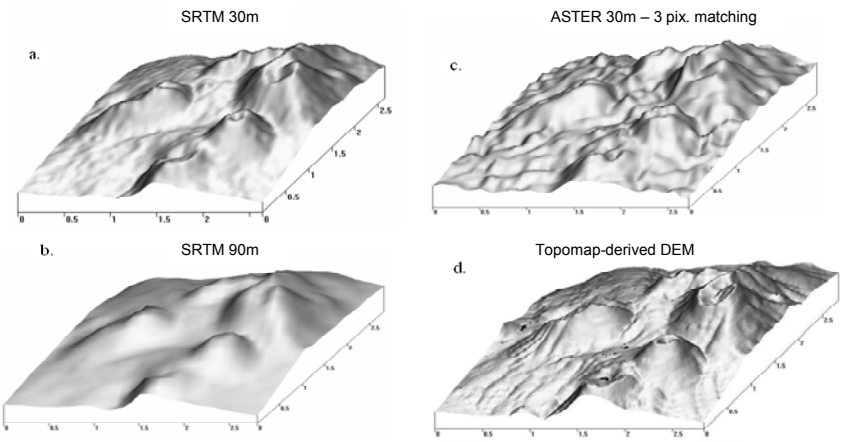

Fig. 2 Oblique view of shaded relief of the MK summit displaying five cinder cones; **(a)** SRTM30; **(b**) SRTM90; **(c**) 30 m resolution ASTER DEM, the stereo-pair of images being matched every 3 pixels; **(d)** 10 m resolution DEM derived from contour lines of the 1:24,000 USGS topomaps.

Identification of factors controlling the largest error allows deriving an average calibration, to relate estimates made on ASTER or SRTM DEMs to corresponding real height values. These calibration values are obtained after selecting the cones for which height estimates are expected to be accurate. Cones with limited height (<20-40 m), located on steep slopes, or with highly irregular cone base were excluded from the datasets for calibration estimation because estimates on these cones suffered from high uncertainties. For horizontal length determinations, any measurement made on SRTM and ASTER DEMs does not need to be corrected systematically, but an uncertainty of $\pm$ 10% is expected due to absence of a sharp break-in-slope at cone base. For vertical measurements, with SRTM30, ASTER and SRTM90, any measurement needs to be corrected by 9.5%, 14% and 27%, respectively. These calibration values correspond to applying an average correction, valid for the range of cone size represented in our sample. The generality of these results could be further evaluated for other volcanic cone fields in future (Kervyn et al., 2006a).

4. Oldoinyo Lengai

The second case study, Oldoinyo Lengai (OL) volcano, illustrates a common situation in geohazard research: the need to derive a high resolution topographic dataset for a region where neither accurate and up-to-date topographic data, nor accurate field validation data are available. OL is an active natro-carbonatite volcano of the East African Rift System (NW Tanzania). It has been continuously emitting lava since 1983 (Kervyn et al., 2006c). Accurate topographic data is essential at OL to map volcano-scale sector collapse deposits and to assess

hazards from future flank instability. Two ASTER scenes, acquired on September 23, 2000 (scene 1), and March 8, 2003 (scene 2), were used to derive DEMs.

4.1. Data processing

No GPS points could be collected in the field due to funding limitations. To calibrate an absolute DEM from the ASTER data, two sets of GPS points provided by independent field parties, were thus combined. The first set of 26 points was acquired with a Leica SR 530 Survey GPS (Differential GPS) on an E-W profile crossing through OL summit. The errors on these points were evaluated at less than 30 cm both horizontally and vertically. The limitation is that data location was not recorded on a topographic map that could be used to locate the data on the ASTER scene. The second set of 63 points was acquired with a hand held GPS (Garmin Etrex Vista) on board a vehicle driving S-N passing along the E base of Lengai. This handheld GPS does not provide a horizontal accuracy better than 3 m and errors in elevation can be as high as ± 10 m (Kervyn et al., 2006a). An "ortho-rectified" Landsat scene was used to locate the GPS points. Such ortho-rectified Landsat image takes into account the sensor characteristics and a global topographic model at 1 km resolution. The low accuracy of the ortho-rectification, especially in steeply dissected terrains, is a source of error for the accurate localization of the GCPs. Although introducing errors into the processing, this was the best available solution to locate the GPS points. From visual matching of the Landsat and ASTER scenes, the GPS points were located on the ASTER stereo-pair.

a. Parameter

	ASTER scene 1 (9 GCPs)			ASTER scene 2 (14 GCPs)		
	Mean	*Standard Deviation*	*RMSE*	*Mean*	*Standard Deviation*	*RMSE*
dX (m)	9.3	7.1	11.4	15.4	13.0	19.9
dY (m)	7.4	6.1	9.4	17.2	14.5	22.2
dZ (m)	6.2	3.0	6.8	7.1	5.3	8.8

b.

GCP	dX (m)	dY (m)	dZ (m)
1	-15.50	2.59	-9.93
2	15.15	-19.64	3.84
3	5.52	-0.981	3.56
4	3.85	-9.43	3.54
5	-2.72	10.66	-9.12
6	-19.54	5.58	6.16
7	-3.86	-3.26	-5.63
8	1.37	12.37	-3.26
9	15.85	2.18	10.87

c.

GCP	dX (m)	dY (m)	dZ (m)
1	12.02	-9.72	-11.73
2	-11.18	-48.67	-4.98
3	-14.56	39.33	1.82
4	0.82	3.97	6.31
5	-13.26	-21.24	7.85
6	8.34	3.16	0.51
7	-13.82	-3.05	5.62
8	-1.92	-3.61	5.05
9	-20.45	-22.25	-9.16
10	26.04	23.56	-4.31
11	49.13	24.55	-3.33
12	-30.98	-11.99	-7.72
13	11.68	1.87	22.50
14	-1.50	24.29	-8.50

Table 2 General (a) and per GCP (b & c) distribution of error in x, y and z for the absolute orientation of the ASTER stereo-pair acquired on September 23, 2000 ((b); scene 1) and March 8, 2003 ((c); scene 2) for OL. The two ASTER scenes were calibrated using a selection of GPS points extracted from 2 independent GPS datasets. For both scenes, the vertical RMS error remains below 10 m.

The relative orientation and the image matching, as evaluated by the software (Virtuozo 3.2), were of good quality thanks to good contrast within the scene. A subset of 9 and 14 GCPs, for scenes 1 and 2, respectively, with a good spatial distribution and producing the smallest RMSE was selected to calibrate the absolute orientation (Table 2). Despite the lack of high quality GPS points located precisely on the ASTER scene at first hand, an average horizontal RMSE of ~10 m and ~20 m and a vertical RMSE of 6 m and 8 m was achieved on the selected GCPs, for scenes 1 and 2, respectively. DEMs at 30 m resolution were extracted.

4.2. Accuracy assessment

Visual inspection of the ASTER DEMs (Fig. 3a) shows that despite the limitations in the calibration process, the resulting DEMs return a realistic representation of the volcano topography. The 2 summit craters and the 2 landslide scarps are identified without ambiguity, as well as several of the largest scoria cones and domes (500-1000 m across; >100 m high). ASTER DEMs are however affected by small-scale noise hindering recognition of true, but small-scale, topographic features, visible on the SRTM DEM (e.g. gullies along OL's flanks). The noise is accounted for by small errors in the image matching process, inducing errors in elevation of 5 to 40 m. Averaging the ASTER DEM to obtain a 90 m resolution significantly reduces the noise affecting the data while enhancing recognition of true topographic features (Figs. 3b and c).

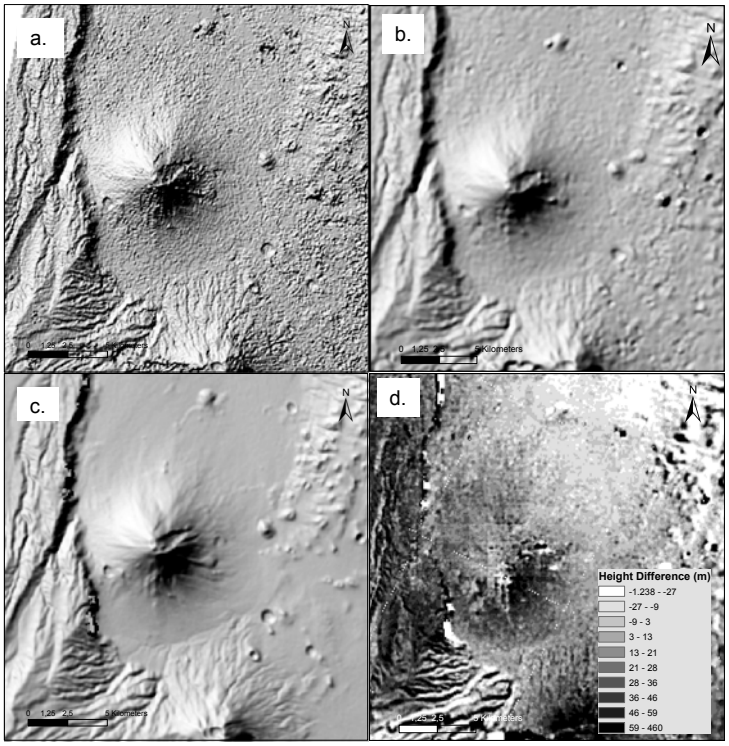

Fig. 3 (a & b) Shaded relief of OL from the ASTER DEM extracted from scene 2 (March 8, 2003) **(a)** at 30 m spatial resolution and **(b)** at 90 m spatial resolution using a 3x3 averaging window. Small-scale artefacts decrease the visual interpretability of the ASTER DEM shaded relief at 30 m, small cones and craters being confused with artefacts; **(c)** shaded relief of the 90 m SRTM DEM that compare well with the ASTER DEM at 90 m, despite lower variability in flat terrains; **(d)** map of elevation difference between the ASTER **(a)** and SRTM **(c)** DEMs. Positive values correspond to a higher elevation in the SRTM DEM.

No high resolution DEM exists over Lengai to assess the absolute accuracy of the SRTM and ASTER DEMs. The two latter datasets were thus compared against each other. When subtracting the ASTER DEMs from the SRTM DEM, average difference values of 17 m and 15.5 m are obtained for scene 1 and 2, respectively. This is in agreement with a systematic offset in elevation observed in the first GPS dataset relative to the SRTM DEM. After correcting for this systematic effect, 50% of the ASTER-derived elevation values are within $\pm$ 20 m of the SRTM estimate. Discrepancies between the ASTER and SRTM DEMs can be attributed to noise in the ASTER DEM and to poorer absolute calibration in areas poorly constrained by GCPs. Relative errors on steep terrains and absolute errors of a few meters can however not be excluded within the SRTM DEM (Rodríguez et al., 2006).

Reduction of the random noise within ASTER DEMs is obtained by averaging DEMs obtained by the independent processing of the two available scenes. After averaging DEMs and correcting for a systematic offset with the SRTM DEM, 50% of the pixels have elevation differences between ASTER and SRTM DEM of less than 15 m. This integration technique shows that errors associated with image matching can be reduced by integrating results from

several ASTER scenes over the same target area. More evolved integration techniques based on the spatial variation of the noise and the quality of the matching process within each DEM will further help to improve the overall accuracy of ASTER-derived DEMs.

When the DEM relative accuracy is assessed by measuring the relative height of different features (Table 3), we find that the estimates on the ASTER and SRTM DEMs are consistent when features are more than 100 m high. Discrepancies are about 10% of the height for 100-200 m high constructs (e.g. phonolite dome; scoria cone) and about 2-4% for higher features (e.g. stratovolcanoes). For constructs smaller than 100 m, discrepancies can be very large and the height estimates are meaningless due to the 90 m resolution of the SRTM DEM and the small-scale artefacts of the ASTER DEM.

Table 3 Relative height of topographic features estimated on the SRTM and ASTER DEMs. Missing data corresponds to features not covered by the DEM extracted from ASTER scene 1 (September 23, 2000).

	Topographic feature	SRTM (m)	ASTER - scene 1 (m)	ASTER - scene 2 (m)
1	*Maar – Tuff ring rim*	2	-10	-8
2	*Debris avalanche block*	20	-3	6
3	*Maar/Pit Crater,*	19	43	41
4	*Scoria cone (N flank of Kerimasi)*	56		55
5	*Maar – Tuff ring rim*	92	84	93
6	*Scoria cone*	70	60	66
7	*Phonolite dome (Oldoinyo Lalarasi)*	114	119	104
8	*Scoria cone (Lalarasi)*	183	163	179
9	*Rift valley wall*	475	441	467
10	*Rift valley wall*	425	356	425
11	*Collapse scar (Kerimasi)*	736		695
12	*Stratovolcano (Kerimasi)*	1104		1066
13	*Stratovolcano (Oldoinyo Lengai)*	1729	1728	1715

5. Discussion and conclusion

The comparative analysis of the accuracy of DEMs provided by ASTER and SRTM allows assessing advantages and limitations of those datasets, prior to using them for retrievals of quantitative estimates of the size of small volcanic features or for understanding of related hazards. The use of ASTER stereo images to derive high resolution DEMs is an efficient alternative when the SRTM is only available at 90 m spatial resolution. ASTER offers the advantage to combine multispectral and topographic datasets acquired simultaneously, and this repetitively, which is of great interest to map and monitor changes in dynamic environments such as volcanoes (Stevens et al., 2004). The major limitation of ASTER data for regular monitoring, as with other optical RS data, is their sensitivity to cloud cover, frequent for high relief sub-tropical volcanoes. The ready-to-be-used SRTM dataset is also of great interest for morphological studies of volcanic terrains, especially for regions with frequent cloud coverage.

OL case study illustrates the limitations of ASTER DEMs when differential GPS data, collected in the field specifically for DEM calibration and accurately indicated on image material, are lacking. The availability, spatial distribution and accuracy of GCPs, which can be precisely located on the ASTER scene, are thus the main factors limiting the accuracy of ASTER DEMs. Without high accuracy calibration data, a realistic representation of the topography can however be obtained with ASTER stereo-pairs. Noise in the ASTER DEM is an issue that can be tackled by integrating DEMs extracted from different ASTER scenes, by reducing the matching resolution or by DEM post-processing (use of smoothing filters). The two latter options however lead to an effective decrease in spatial resolution.

Although these limitations result in lower absolute and relative vertical accuracies of the ASTER-derived DEM compared to 30 m SRTM, it still provides an accurate representation of the overall volcano morphology. The height of small-scale volcanic features can be estimated

with a relatively good accuracy (average underestimation of 20% of cone height), when the ASTER DEM is constrained by high quality GCPs, with the exception of deeply-dissected or low spectral contrast terrain.

Acknowledgments. *M.K. and G.G.J.E. thank the Belgian NSF (Fonds voor Wetenschappelijk Onderzoek-Vlaanderen) and the "Fondation Belge de la Vocation" for support. The ASTER and SRTM imagery were provided by the LPDAAC, USGS, Department of Interior and the Jet Propulsion Laboratory, respectively*

REFERENCES

Hirano, A., Welch, R. & Lang, H. 2003. Mapping from ASTER stereo image data: DEM validation and accuracy assessment. *ISPRS Journal of Photogrammetry & Remote Sensing*, **57**, 356-370.

Kervyn, M., Goossens, R., Jacobs, P. & Ernst, G.G.J. 2006a. Mapping volcano topography with remote sensing: ASTER vs SRTM. *International Journal of Remote Sensing*, **xxx (submitted)**.

Kervyn, M., Kervyn, F., Goossens, R., Rowland, S.K. & Ernst, G.G.J. 2006b. Mapping volcanic terrain using high-resolution and 3D remote sensing. *Geological Society of London Special Publication*, **in press**.

Kervyn, M., Harris, A.J.L., Belton, F., Mbede, E., Jacobs, P. & Ernst, G.G.J. 2006c. Thermal remote sensing of the low-intensity thermal anomalies of Oldoinyo Lengai, Tanzania. *International Journal of Remote Sensing*, **xxx (submitted)**.

Pieri, D. & Abrams, M.J. 2004. ASTER watches the world's volcanoes: A new paradigm for volcanological observations from orbit. *Journal of Volcanology and Geothermal Research*, **135**, 13-28.

Riedel, C., Ernst, G.G.J. & Riley, M. 2003. Controls on the growth and geometry of pyroclastic constructs. *Journal of Volcanology and Geothermal Research*, **127**, 121-152.

Rodríguez, E., Morris, C.S. & Belz, J.E. 2006. A global assessment of the SRTM performance. *Photogrammetric Engineering and Remote Sensing*, **72**, 249-260.

Simkin, T. & Siebert, L. 1994. *Volcanoes of the World*. Tucson, (2nd edition), Geosciences Press, 349 pp.

Stevens, N.F., Manville, V. & Heron, D.W. 2002. The sensitivity of a volcanic flow model to digital elevation model accuracy: Experiments with digitised map contours and interferometric SAR at Ruapehu and Taranaki volcanoes, New Zealand. *Journal of Volcanology and Geothermal Research*, **119**, 89-105.

Stevens, N.F., Garbeil, H. & Mouginis-Mark, P.J. 2004. NASA EOS Terra ASTER: Volcanic topographic mapping and capability. *Remote Sensing of Environment*, **90**, 405-414.